Preprints of the 21st IFAC World Congress (Virtual)
Berlin, Germany, July 12-17, 2020

Compliance Control for Robust Assembly with Redundant Manipulators

Kim D. Listmann * **Florian Hans** ** **Arne Wahrburg** ***

* *ABB Future Labs Switzerland, (e-mail: kim.listmann@ch.abb.com)*
** *TU Braunschweig, Institute of Control Engineering, (e-mail: florian.hans@tu-bs.de)*
*** *ABB Corporate Research Center Germany, (e-mail: arne.wahrburg@de.abb.com)*

Abstract: Given the problem of static and dynamic contact stability of manipulators, this work extends classical hybrid force/motion control by introducing an additional feedback part to allow smooth environmental contact of the robot. The extension is the outcome of an in-depth stability analysis of velocity-controlled manipulators in passive environments and can be considered the first of its kind. In addition to this theoretical contribution, the application to a redundant 7-DoF robot confirms the achievable benefit compared to the classical implementation w.r.t. transient effects (like positional deviation or exerted force) in the event of an environmental contact.

Keywords: Hybrid force/motion control, redundant manipulators, impedance control, unstructured environments, stability analysis.

1. INTRODUCTION

For decades robots have been used on the shop floor of factories. So far, their main purpose was to automatically perform a given task, e.g., welding, dispensing, pick & place applications etc. Independent of the specific application, the foremost goal always was to precisely follow a prescribed trajectory (e.g. dispensing) or to optimally execute a certain motion and boost task productivity (e.g. butterfly-like pick & place operation) (Brogårdh, 2009). Thus, the robot performance is dominated by a pure motion task. Such tasks have been performed behind fences to avoid direct interaction with the operator, mainly for safeguarding reasons. For applications requiring force-based interaction, a strategy known as hybrid force/motion control (Craig and Raibert, 1979) is mostly applied in industrial manipulators. Some Cartesian directions are controlled using standard position control approaches, whereas the remaining (orthogonal) Cartesian directions are governed by an admittance-type indirect force controller (Hogan, 1985).

With the advent of an ever-closer collaboration between humans and robots, recently developed as HRC (Human-robot collaboration) (Krüger et al., 2009; Thomas et al., 2016), this set-up seems inappropriate. Firstly, this is because its transient behavior in the conversion from free motion to force-guided contact is hard to predict and difficult to always ensure stability using the simple hybrid control approach (Fisher and Mujtaba, 1992). Secondly, due to the rise of HRC, the number of intended environmental interactions between humans (as part of the environment of the robot) and robots will increase significantly (Thomas et al., 2016). Hence, manipulator applications transform from a motion- to an interaction-dominated world.

Several force control approaches have been developed to meet the requirements of interaction scenarios (see (Siciliano and Khatib, 2016) and (Zeng and Hemami, 1997) for an overview). Generally, the control schemes can be categorized into direct and indirect approaches (Siciliano and Villani, 1999) while indirect force control can in turn be subdivided into impedance and admittance (Ott et al., 2010). For interaction tasks in highly unstructured environments, impedance-based schemes benefit from their stability properties in contact and contact-loss situations (Schindlbeck and Haddadin, 2015). On the contrary, force-controlled tasks requiring very high positioning accuracy in position-controlled directions (cf. (Jonsson et al., 2013)), hybrid force/motion schemes relying on admittance control still have a high potential.

Based on this motivation, this work proposes an extension of the traditional hybrid control scheme. We follow up on (Fisher and Mujtaba, 1992), which in turn extended the original hybrid concept proposed in (Craig and Raibert, 1979) and we present a new perspective on the problem of kinematic instability. Our results are based on a detailed dynamical stability analysis of the position-controlled manipulator in free motion as well as the force-controlled manipulator in contact with the environment. The contribution is three-fold: i) we apply a corrected transformation to properly update the hybrid control structure itself, ii) an additional feedback is introduced for robust stabilization of the scheme and iii) a constructive method for the design of all control gains is proposed, resulting in a well-tuned closed-loop behavior for robots interacting with the environment.

To this end, the paper is organized as follows: In the next section, the general hybrid force/motion control approach is introduced together with common terminology used throughout the paper. Section 3 describes the problem at hand to be studied in detail in the remainder of the paper. The main results are presented in Section 4 and can be divided into the derivation of the proposed extension of the scheme, its stability analysis and a structured design methodology for the tuning. An application to ABB's dual-arm robot YuMi® is provided in Section 5 by performing a force-controlled motion task in a compliant environment. Finally, a conclusion is provided in Section 6.

2. BACKGROUND

2.1 System Description

The joint space dynamics of a rigid manipulator with n joints and coordinates $\boldsymbol{q} \in \mathbb{R}^n$ can be written as

$$\boldsymbol{M}(\boldsymbol{q})\ddot{\boldsymbol{q}} + \boldsymbol{C}(\boldsymbol{q}, \dot{\boldsymbol{q}})\dot{\boldsymbol{q}} + \boldsymbol{g}(\boldsymbol{q}) = \boldsymbol{\tau} - \boldsymbol{\tau}_{\text{ext}}. \tag{1}$$

Herein, $\boldsymbol{M}(\boldsymbol{q}) \in \mathbb{R}^{n\times n}$ is the inertia matrix of the robot, $\boldsymbol{C}(\boldsymbol{q}, \dot{\boldsymbol{q}}) \in \mathbb{R}^{n\times n}$ is the matrix containing factorized Coriolis and centrifugal terms, and the vector $\boldsymbol{g}(\boldsymbol{q}) \in \mathbb{R}^n$ represents the gravity torques. The motor torques $\boldsymbol{\tau} \in \mathbb{R}^n$ are considered as the manipulator control input, and $\boldsymbol{\tau}_{\text{ext}} \in \mathbb{R}^n$ is the vector of joint torques associated with external forces exerted from the robot end-effector on the environment.

The forward kinematics relate the joint coordinate vector $\boldsymbol{q}$ with the Cartesian posture vector of the end-effector $\boldsymbol{x} \in \mathbb{R}^m$, and is given by the mapping $\boldsymbol{x} := \mathcal{K}(\boldsymbol{q})$, $\mathcal{K} : \mathbb{R}^n \mapsto \mathbb{R}^m$. Accordingly, the differential kinematics for the Cartesian end-effector velocities are given by

$$\dot{\boldsymbol{x}} = \boldsymbol{J}(\boldsymbol{q})\dot{\boldsymbol{q}}, \quad \boldsymbol{J}(\boldsymbol{q}) = \frac{\partial \mathcal{K}(\boldsymbol{q})}{\partial \boldsymbol{q}}, \tag{2}$$

where $\boldsymbol{J}(\boldsymbol{q}) \in \mathbb{R}^{m\times n}$ is the Jacobian matrix.

For all manipulators with $n \geq m$, the differential kinematics (2) can be treated as a system of (linear) equations of the form $\boldsymbol{A}\boldsymbol{\chi} = \boldsymbol{\beta}$, with $\boldsymbol{A} \equiv \boldsymbol{J}(\boldsymbol{q})$. Then, all solutions $\boldsymbol{\chi} = \dot{\boldsymbol{q}}$ are parametrized by

$$\dot{\boldsymbol{q}} = \boldsymbol{J}^\dagger(\boldsymbol{q})\dot{\boldsymbol{x}} + \left[\boldsymbol{I} - \boldsymbol{J}^\dagger(\boldsymbol{q})\boldsymbol{J}(\boldsymbol{q})\right]\boldsymbol{\zeta}, \tag{3}$$

where $\boldsymbol{J}^\dagger(\boldsymbol{q}) \in \mathbb{R}^{n\times m}$ is any pseudoinverse of $\boldsymbol{J}(\boldsymbol{q})$, satisfying $\boldsymbol{J}(\boldsymbol{q})\boldsymbol{J}^\dagger(\boldsymbol{q})\boldsymbol{J}(\boldsymbol{q}) = \boldsymbol{J}(\boldsymbol{q})$, $\forall \boldsymbol{q} \in \mathbb{R}^n$ and $\boldsymbol{\zeta} \in \mathbb{R}^n$ is an arbitrary vector that is projected onto the null space of the Jacobian, i.e., $\left[\boldsymbol{I} - \boldsymbol{J}^\dagger(\boldsymbol{q})\boldsymbol{J}(\boldsymbol{q})\right]\boldsymbol{\zeta} \in \ker(\boldsymbol{J})$. Given (3), it is convenient to use the unique Moore-Penrose-pseudoinverse, which is denoted with a superscript $+$, as a special case of a generalized (right) inverse (Serre, 2010). Therefore, if motion or velocity related quantities are considered, the Moore-Penrose-pseudoinverse $\boldsymbol{J}^+(\boldsymbol{q})$ is used in the remainder of the article, i.e., $\boldsymbol{J}^\dagger(\boldsymbol{q}) = \boldsymbol{J}^+(\boldsymbol{q})$.

Similarly to the differential kinematics and its inverse relation, the relationship between joint torques $\boldsymbol{\tau}_{\text{ext}}$ and external operational forces $\boldsymbol{f}_{\text{ext}} \in \mathbb{R}^m$ at the end-effector is given by

$$\boldsymbol{\tau}_{\text{ext}} = \boldsymbol{J}^T(\boldsymbol{q})\boldsymbol{f}_{\text{ext}} + \left[\boldsymbol{I} - \boldsymbol{J}^T(\boldsymbol{q})\boldsymbol{J}^{T\dagger}(\boldsymbol{q})\right]\boldsymbol{\varsigma}, \tag{4}$$

where $\boldsymbol{J}^T(\boldsymbol{q})\boldsymbol{f}_{\text{ext}}$ represents joint torques that are associated with forces acting at the end-effector and

$$\left[\boldsymbol{I} - \boldsymbol{J}^T(\boldsymbol{q})\boldsymbol{J}^{T\dagger}(\boldsymbol{q})\right]\boldsymbol{\varsigma} \in \ker(\boldsymbol{J^T}),\ \boldsymbol{\varsigma} \in \mathbb{R}^m$$

takes internal motions into account. To avoid motions in the null space that produce any acceleration of the end-effector in the Cartesian space, the transposed generalized inverse $\boldsymbol{J}^{T\dagger}(\boldsymbol{q})$ has to be dynamically consistent, satisfying $\boldsymbol{J}(\boldsymbol{q})\boldsymbol{M}^{-1}(\boldsymbol{q})\left[\boldsymbol{I} - \boldsymbol{J}^T(\boldsymbol{q})\boldsymbol{J}^{T\dagger}(\boldsymbol{q})\right]\boldsymbol{\varsigma} = \boldsymbol{0}$ (Khatib, 1995). Hence, if Cartesian forces are mapped to joint torques, the unique dynamically consistent (left) inverse $\boldsymbol{J}^{T\#}(\boldsymbol{q}) \in \mathbb{R}^{m\times n}$ is used, i.e., (Khatib, 1995)

$$\begin{aligned}\boldsymbol{J}^{T\#}(\boldsymbol{q}) &= \boldsymbol{J}^{T\dagger}(\boldsymbol{q}) \\ &= \left(\boldsymbol{J}(\boldsymbol{q})\boldsymbol{M}^{-1}(\boldsymbol{q})\boldsymbol{J}^T(\boldsymbol{q})\right)^{-1}\boldsymbol{J}(\boldsymbol{q})\boldsymbol{M}^{-1}(\boldsymbol{q}).\end{aligned} \tag{5}$$

2.2 Hybrid Force/Motion Control

Most of the present industrial manipulators are equipped with independent joint-level PID controllers (Siciliano and Khatib, 2016) or use some other kind of cascaded position control structure for motion control tasks. If besides pure motion control, operating forces are required, hybrid force/motion control schemes are a traditional approach(Craig and Raibert, 1979).

A diagonal selection matrix $\boldsymbol{S} \in \mathbb{R}^{m\times m}$ is employed to specify which directions are force-controlled (corresponding element in $\boldsymbol{S}$ is 1) and which are position controlled (diagonal element in $\boldsymbol{S}$ is 0). We further introduce $\boldsymbol{S}^\perp = (\boldsymbol{I} - \boldsymbol{S})$, where $\boldsymbol{I} \in \mathbb{R}^{m\times m}$ is the identity matrix.

The desired manipulator joint configuration $\boldsymbol{q}_{\text{d}}(t) \in \mathbb{R}^n$ is regulated by n proportional controllers, given by the gain matrix $\boldsymbol{K}_{\text{p}} \in \mathbb{R}_+^{n\times n}, \boldsymbol{K}_{\text{p}} = \text{diag}\{K_{\text{p},1}, \ldots, K_{\text{p},n}\}$. In order to select the joints according to the specified position-controlled directions in Cartesian space, the joint error $\boldsymbol{q}_{\text{e}} \in \mathbb{R}^n, \boldsymbol{q}_{\text{e}} = \boldsymbol{q}_{\text{d}}(t) - \boldsymbol{q}$ is transformed to $\boldsymbol{q}_{\text{eS}^\perp} \in \mathbb{R}^n$ using $\boldsymbol{J}^+(\boldsymbol{q})\boldsymbol{S}^\perp\boldsymbol{J}(\boldsymbol{q})$. Basically, the usage of the Jacobian $\boldsymbol{J}(\boldsymbol{q})$ realizes a mapping onto Cartesian space in terms of a first order approximation that transforms differential motions in joint space $\boldsymbol{q}$ to differential displacements in Cartesian space $\boldsymbol{x}$. The pseudoinverse $\boldsymbol{J}^+(\boldsymbol{q})$ accomplishes a mapping (back) to joint space. Therefore, the matrix $\boldsymbol{J}^+(\boldsymbol{q})\boldsymbol{S}^\perp\boldsymbol{J}(\boldsymbol{q})$ can be understood as a selection matrix in joint space.

Additionally, a proportional controller with gain matrix $\boldsymbol{D}^{-1} \in \mathbb{R}^{m\times m}$ acts as an outer loop force controller on the Cartesian force error $\boldsymbol{f}_{\text{e}} \in \mathbb{R}^m, \boldsymbol{f}_{\text{e}} = \boldsymbol{f}_{\text{d}}(t) - \boldsymbol{f}_{\text{ext}}$ between desired forces $\boldsymbol{f}_{\text{d}}(t) \in \mathbb{R}^m$ and actual forces $\boldsymbol{f}_{\text{ext}}$ defined in the robot base frame. This proportional controller $\boldsymbol{D}^{-1}$ represents an admittance in terms of the basic idea of impedance control, proposed by Hogan (Hogan, 1985). Hence, $\boldsymbol{D}$ is referred to as damping matrix throughout this work.

Given the force controller output, $\dot{\boldsymbol{x}}_{\text{e}}$ is mapped to joint space using the transformation matrix $\boldsymbol{J}^+(\boldsymbol{q})\boldsymbol{S}$, which simultaneously takes the specified force-controlled directions in Cartesian space into account.

The aggregated reference joint velocities $\dot{\boldsymbol{q}}_{\text{r}}(t) = \dot{\boldsymbol{q}}_{\text{p}}(t) + \dot{\boldsymbol{q}}_{\text{f}}(t)$ with $\dot{\boldsymbol{q}}_{\text{r}}(t) \in \mathbb{R}^n$ serve as control input of the underlying velocity-controlled manipulator. Here, $\dot{\boldsymbol{q}}_{\text{p}}(t) \in \mathbb{R}^n$ and $\dot{\boldsymbol{q}}_{\text{f}}(t) \in \mathbb{R}^n$ represent the velocity components associated with the position- and force-controlled parts, respectively. Referring to the control objectives in robot manipulation applications and to independent joint control (or decentralized control) (Spong and Vidyasagar, 2008), where each manipulator joint is considered as a single-input/single-output (SISO) system, the velocity-controller is tuned to accomplish well damped and sufficiently fast joint velocity movements. Thus, the input-output behavior of the velocity-controlled manipulator is modeled as

$$\boldsymbol{T}_{\mathrm{VR}}\ddot{\boldsymbol{q}} + \dot{\boldsymbol{q}} = \dot{\boldsymbol{q}}_{\mathrm{r}}, \tag{6}$$

with the diagonal matrix $\boldsymbol{T}_{\mathrm{VR}} = \mathrm{diag}\{T_{\mathrm{VR},1}, \ldots, T_{\mathrm{VR},n}\} \in \mathbb{R}_{+}^{n\times n}$ containing the equivalent time constants, respectively, and $\dot{\boldsymbol{q}}_{\mathrm{r}}$ as reference control input. Measurements show that this is a reasonable assumption (Hans, 2015).

Remark 1. In contrast to the described structure, the original hybrid control scheme of Craig and Raibert (1979) implements a force controller in joint space. The reference torques for non-redundant manipulators are calculated using the transposed Jacobian $\boldsymbol{J}^T(\boldsymbol{q})$ and the relation $\boldsymbol{\tau}_{\mathrm{ext}} = \boldsymbol{J}^T(\boldsymbol{q})\boldsymbol{f}_{\mathrm{ext}}$ maps exerted Cartesian forces to the joint space.

3. PROBLEM STATEMENT

During their research, An and Hollerbach (1987) experienced that some hybrid force control structures become unstable dependent on their (kinematic) configuration only. In An and Hollerbach (1987), the authors investigated how an exemplary two-joint-manipulator that implements a hybrid control scheme shows an unstable behavior.

Later, Fisher and Mujtaba (1992) found that the original hybrid force/motion control scheme developed by Craig and Raibert (1979) is based on the incomplete and inappropriate mathematical formulation $\boldsymbol{q}_{\mathrm{eS}^{\perp}} = \boldsymbol{J}^{+}(\boldsymbol{q})\boldsymbol{S}^{\perp}\boldsymbol{J}(\boldsymbol{q})\boldsymbol{q}_{\mathrm{e}}$. Following basic lines of reasoning, Fisher introduced the concept of kinematic stability and proposed sufficient criteria that can be used to analyze robotic systems with respect to kinematic stability properties without requiring a complete dynamical system analysis.

From a control engineering point of view, kinematic stability is related to the input/output stability of dynamic systems. Depending on the manipulator configuration, the presence of a Cartesian selection matrix $\boldsymbol{S}$ (or $\boldsymbol{S}^{\perp}$), associated with the mappings from and into the joint space, could cause a positive feedback or violate the small gain theorem (Khalil, 2001), thus resulting in an unbounded output. It should be highlighted that kinematic stability does not imply dynamic stability. Conversely, the system can show an unstable behavior (at certain operating points) if the kinematic stability conditions are violated, but can still be stable locally. The proposed kinematic stability criteria rather impose requirements on the joint space transformation that relate the vector $\boldsymbol{q}_{\mathrm{e}}$ to the vector $\boldsymbol{q}_{\mathrm{eS}^{\perp}}$ omitting the closed-loop system dynamics.

Similar to the example in An and Hollerbach (1987), the unstable behavior of a manipulator implementing the hybrid scheme can be illustrated considering a robot moving in the unconstrained space, i.e., in free motion, where $\boldsymbol{f}_{\mathrm{ext}} = \boldsymbol{0}$. For convenience, it is supposed that the velocity controller is well tuned, whereby the dynamics of the velocity-controlled manipulator can be treated as n decoupled first order lag systems of the form (6). Introducing the state variable $\left[\boldsymbol{e}_{\mathrm{q}}^T, \dot{\boldsymbol{e}}_{\mathrm{q}}^T\right]^T \in \mathbb{R}^{2n}$, where $\boldsymbol{e}_{\mathrm{q}} = \boldsymbol{q} - \boldsymbol{q}_{\mathrm{d}}$ is the error between the actual configuration $\boldsymbol{q}$ and some constant desired position $\boldsymbol{q}_{\mathrm{d}}$, the residual dynamics of the manipulator in free motion with $\boldsymbol{f}_{\mathrm{ext}} = \boldsymbol{0}$ and position controller $\boldsymbol{K}_{\mathrm{P}}\boldsymbol{J}^{+}(\boldsymbol{q})\boldsymbol{S}^{\perp}\boldsymbol{J}(\boldsymbol{q})$ can be formulated in state space representation as

$$\frac{d}{dt}\begin{bmatrix}\boldsymbol{e}_{\mathrm{q}}\\ \dot{\boldsymbol{e}}_{\mathrm{q}}\end{bmatrix} = \begin{bmatrix}\dot{\boldsymbol{e}}_{\mathrm{q}}\\ -\boldsymbol{T}_{\mathrm{VR}}^{-1}\left(\boldsymbol{K}_{\mathrm{P}}\boldsymbol{J}^{+}(\boldsymbol{q})\boldsymbol{S}^{\perp}\boldsymbol{J}(\boldsymbol{q})\boldsymbol{e}_{\mathrm{q}} + \dot{\boldsymbol{e}}_{\mathrm{q}}\right)\end{bmatrix}, \tag{7}$$

in case the null space component is omitted by choosing $\boldsymbol{\zeta} = \boldsymbol{0}$. Considering small changes of the state variable, $\left[(\Delta\boldsymbol{e}_{\mathrm{q}})^T, (\Delta\dot{\boldsymbol{e}}_{\mathrm{q}})^T\right]^T$ around the equilibrium / operating point $\boldsymbol{e}_{\mathrm{q}}^{*} = \boldsymbol{0}$, $\dot{\boldsymbol{e}}_{\mathrm{q}}^{*} = \boldsymbol{0}$, the linearization

$$\begin{bmatrix}\Delta\dot{\boldsymbol{e}}_{\mathrm{q}}\\ \Delta\ddot{\boldsymbol{e}}_{\mathrm{q}}\end{bmatrix} = \underbrace{\begin{bmatrix}\boldsymbol{0} & \boldsymbol{I}\\ -\boldsymbol{T}_{\mathrm{VR}}^{-1}\boldsymbol{K}_{\mathrm{P}}\boldsymbol{J}^{+}(\boldsymbol{q}_{\mathrm{d}})\boldsymbol{S}^{\perp}\boldsymbol{J}(\boldsymbol{q}_{\mathrm{d}}) & -\boldsymbol{T}_{\mathrm{VR}}^{-1}\end{bmatrix}}_{=:\boldsymbol{\Gamma}_{\mathrm{J+S^{\perp}J}}}\begin{bmatrix}\Delta\boldsymbol{e}_{\mathrm{q}}\\ \Delta\dot{\boldsymbol{e}}_{\mathrm{q}}\end{bmatrix} \tag{8}$$

can be calculated substituting $\boldsymbol{J}(\boldsymbol{q}) := \boldsymbol{J}(\boldsymbol{e}_{\mathrm{q}} + \boldsymbol{q}_{\mathrm{d}})$.

To guarantee (local) stability of the linear system (8) at the operating point, the eigenvalues of the system matrix $\boldsymbol{\Gamma}_{\mathrm{J+S^{\perp}J}}$ must lie in the open left half plane. Otherwise, referring to the indirect method of Lyapunov (Khalil, 2001), if at least one eigenvalue lies in the open right half plane, the equilibrium point of both the linearized and the nonlinear system is unstable. Note that for robots this is posture dependent [1].

As emphasized, it is not guaranteed that the examined velocity-based hybrid control scheme results in a stable closed-loop system for any non-singular configuration. As a consequence, in the next section, a modification of the structure is proposed and proven to be stable in the sense of Lyapunov.

4. MAIN RESULTS

Based on the suggestions of Fisher concerning the modification of the position-controlled part of the original hybrid control scheme (Fisher and Mujtaba, 1992), the examined velocity-based control structure can be corrected to result in a kinematically stable system.

Starting with the differential kinematics (2) and left-multiplying the selection matrix $\boldsymbol{S}$, the force/velocity related equation can be defined as

$$\dot{\boldsymbol{x}}_{\mathrm{eS}} = \boldsymbol{S}\dot{\boldsymbol{x}}_{\mathrm{e}} = \boldsymbol{S}\boldsymbol{J}(\boldsymbol{q})\dot{\boldsymbol{q}}_{\mathrm{eS}}. \tag{9}$$

Interpreting (9) as a system of (linear) equations of the form $\boldsymbol{A}\boldsymbol{\chi} = \boldsymbol{\beta}$, with $\boldsymbol{A} \equiv \boldsymbol{S}\boldsymbol{J}(\boldsymbol{q})$ and $\boldsymbol{\chi} \equiv \dot{\boldsymbol{q}}_{\mathrm{eS}}$ as unknown vector, the general inverse solution is given by

$$\dot{\boldsymbol{q}}_{\mathrm{g,eS}} = (\boldsymbol{S}\boldsymbol{J}(\boldsymbol{q}))^{+}\dot{\boldsymbol{x}}_{\mathrm{eS}} + \left[\boldsymbol{I} - (\boldsymbol{S}\boldsymbol{J}(\boldsymbol{q}))^{+}(\boldsymbol{S}\boldsymbol{J}(\boldsymbol{q}))\right]\boldsymbol{\zeta}, \tag{10}$$

which is denoted with a subscript g. Similarly, using the Jacobian $\boldsymbol{J}(\boldsymbol{q})$ as differential motion transformation, the position related equation is given by

$$\boldsymbol{x}_{\mathrm{eS}^{\perp}} = \boldsymbol{S}^{\perp}\boldsymbol{x}_{\mathrm{e}} = \boldsymbol{S}^{\perp}\boldsymbol{J}(\boldsymbol{q})\boldsymbol{q}_{\mathrm{eS}^{\perp}}, \tag{11}$$

with the general solution (Fisher and Mujtaba, 1992)

$$\boldsymbol{q}_{\mathrm{g,eS}^{\perp}} = (\boldsymbol{S}^{\perp}\boldsymbol{J}(\boldsymbol{q}))^{+}\boldsymbol{x}_{\mathrm{eS}^{\perp}} + \left[\boldsymbol{I} - (\boldsymbol{S}^{\perp}\boldsymbol{J}(\boldsymbol{q}))^{+}(\boldsymbol{S}^{\perp}\boldsymbol{J}(\boldsymbol{q}))\right]\boldsymbol{\zeta}.$$

Remark 2. Considering the force/velocity related equations (9), it is mathematically incorrect to omit the effect of $\boldsymbol{S}$ on the Jacobian $\boldsymbol{J}(\boldsymbol{q})$ on the right hand side of (9) and develop the inverse matrix $\boldsymbol{J}^{+}(\boldsymbol{q})\boldsymbol{S}$. The matrix $\boldsymbol{S}\boldsymbol{J}(\boldsymbol{q}), \boldsymbol{S} \neq \boldsymbol{I}$ represents a singular matrix with a reduced rank. In fact, the premultiplication with $\boldsymbol{S}$ in (9) reduces the dimension of the image space of the respective mapping and the transformation matrix $\boldsymbol{S}\boldsymbol{J}(\boldsymbol{q})$ maps the redundant manipulator joints $\dot{\boldsymbol{q}}_{\mathrm{eS}}$ onto this reduced image space. The

[1] Think of a three-link planar manipulator with "elbow-up" (stable) or "elbow-down" (unstable) configuration.

same holds true for the position related equations (11). As a consequence, the present derivation corrects this flaw in the derivation of hybrid force/motion control schemes.

4.1 Modified Hybrid Force/Motion Control Scheme

Concerning the general force/velocity and position related equations (10) and (4), we suggest the inverse relations

$$\dot{\boldsymbol{q}}_{\mathrm{eS}} = (\boldsymbol{S}\boldsymbol{J}(\boldsymbol{q}))^{+}\dot{\boldsymbol{x}}_{\mathrm{eS}} + \left[\boldsymbol{I} - \boldsymbol{J}(\boldsymbol{q})^{+}\boldsymbol{J}(\boldsymbol{q})\right]\boldsymbol{\zeta}, \tag{12a}$$

$$\boldsymbol{q}_{\mathrm{eS}^{\perp}} = (\boldsymbol{S}^{\perp}\boldsymbol{J}(\boldsymbol{q}))^{+}\boldsymbol{x}_{\mathrm{eS}^{\perp}}, \tag{12b}$$

to transform the Cartesian velocity/position errors $\dot{\boldsymbol{x}}_{\mathrm{eS}}$, $\boldsymbol{x}_{\mathrm{eS}^{\perp}}$ that are associated with the selected Cartesian directions into (selected) joint variables $\dot{\boldsymbol{q}}_{\mathrm{eS}}$, $\boldsymbol{q}_{\mathrm{eS}}$. Herein, the unique minimum Euclidean norm solutions of (10) and (4) are considered as well as an additional orthogonal component $[\boldsymbol{I} - \boldsymbol{J}(\boldsymbol{q})^{+}\boldsymbol{J}(\boldsymbol{q})]\,\boldsymbol{\zeta}$ to explicitly allow null space motions in case of redundant manipulators ($n > m$).

Using (12), the modified velocity-based hybrid force/ motion control scheme of Fig. 1 is proposed.

The proposed structure utilizes the idea of Craig and Raibert (1979) to feed back the Cartesian end-effector posture $\boldsymbol{x}$ instead of joint variables $\boldsymbol{q}$. By doing this, all reference signals can be defined in Cartesian space. Hence, more intuitive strategies for the trajectory planning in Cartesian space can be considered. Alternatively, an equivalent joint variable feedback can be implemented using the Jacobian $\boldsymbol{J}(\boldsymbol{q})$ as differential motion transformation, yielding $\boldsymbol{q}_{\mathrm{eS}^{\perp}} = (\boldsymbol{S}^{\perp}\boldsymbol{J}(\boldsymbol{q}))^{+}(\boldsymbol{S}^{\perp}\boldsymbol{J}(\boldsymbol{q}))\boldsymbol{q}_{\mathrm{e}}$.

As can be observed from Fig. 1, an additional feedback part within the force-controlled part is introduced. The proportional controller $\boldsymbol{P} \in \mathbb{R}^{m\times m}$ amplifies (or reduces) the current end-effector velocity $\dot{\boldsymbol{x}} = \boldsymbol{J}(\boldsymbol{q})\dot{\boldsymbol{q}}$.

Remark 3. Admittance control can be implemented setting $(\boldsymbol{S}^{\perp}\boldsymbol{J}(\boldsymbol{q}))^{+} = \boldsymbol{J}^{+}(\boldsymbol{q})$ or $(\boldsymbol{S}^{\perp}\boldsymbol{J}(\boldsymbol{q}))^{+}(\boldsymbol{S}^{\perp}\boldsymbol{J}(\boldsymbol{q})) = \boldsymbol{I}$, respectively.

4.2 Dynamical Stability

Stability of Manipulator in Free Motion In order to show the dynamical stability of the manipulator in free motion, i.e., $\boldsymbol{f}_{\mathrm{ext}} = \boldsymbol{0}$, the residual dynamics of the position-controlled robot (6) in joint space are considered. Defining the state variable $\left[\boldsymbol{e}_{\mathrm{q}}^{\top}, \dot{\boldsymbol{e}}_{\mathrm{q}}^{\top}\right]^{\top} \in \mathbb{R}^{2n}$ with the (time-dependent) error $\boldsymbol{e}_{\mathrm{q}} = \boldsymbol{q} - \boldsymbol{q}_{\mathrm{d}}(t)$, similar to (7), the residual closed-loop dynamics in state space representation are given by

$$\frac{d}{dt}\begin{bmatrix}\boldsymbol{e}_{\mathrm{q}}\\ \dot{\boldsymbol{e}}_{\mathrm{q}}\end{bmatrix} = \begin{bmatrix}\dot{\boldsymbol{e}}_{\mathrm{q}}\\ -\boldsymbol{T}_{\mathrm{VR}}^{-1}\left(\boldsymbol{K}_{\mathrm{P}}(\boldsymbol{S}^{\perp}\boldsymbol{J})^{+}(\boldsymbol{S}^{\perp}\boldsymbol{J})\boldsymbol{e}_{\mathrm{q}} + \dot{\boldsymbol{e}}_{\mathrm{q}}\right)\end{bmatrix}, \tag{13}$$

where the substitution $\boldsymbol{J}(\boldsymbol{e}_{\mathrm{q}}, t) := \boldsymbol{J}(\boldsymbol{e}_{\mathrm{q}} + \boldsymbol{q}_{\mathrm{d}}(t)) = \boldsymbol{J}(\boldsymbol{q})$ is utilized and no null space tasks are specified, i.e., $\boldsymbol{\zeta} = \boldsymbol{0}$.

As a prerequisite, it is assumed in the following sections that the desired trajectory $\boldsymbol{q}_{\mathrm{d}}(t) \in \overline{\mathbb{Q}}_{\mathrm{R}} \subset \mathbb{R}^{n}$ is continuously differentiable and defined such that only nonsingular postures are contained (i.e. bounded velocities). Moreover, in some equations, time- and state-dependencies are omitted for brevity but should be kept in mind.

Applying Lyapunov stability theory for non-autonomous systems, the continuous differentiable (time-invariant) Lyapunov function candidate $V_{\mathrm{p}}(\boldsymbol{e}_{\mathrm{q}}, \dot{\boldsymbol{e}}_{\mathrm{q}}) : \overline{\mathbb{Q}}_{\mathrm{R}} \times \mathbb{R}^{n} \mapsto \mathbb{R}$

$$V_{\mathrm{p}} = \frac{1}{2}\begin{bmatrix}\boldsymbol{e}_{\mathrm{q}}\\ \dot{\boldsymbol{e}}_{\mathrm{q}}\end{bmatrix}^{\top}\begin{bmatrix}\alpha_1\boldsymbol{K}_{\mathrm{P}}^{-1} & \alpha_1\boldsymbol{K}_{\mathrm{P}}^{-1}\boldsymbol{T}_{\mathrm{VR}}\\ \alpha_1(\boldsymbol{K}_{\mathrm{P}}^{-1}\boldsymbol{T}_{\mathrm{VR}})^{\top} & \boldsymbol{K}_{\mathrm{P}}^{-1}\boldsymbol{T}_{\mathrm{VR}}\end{bmatrix}\begin{bmatrix}\boldsymbol{e}_{\mathrm{q}}\\ \dot{\boldsymbol{e}}_{\mathrm{q}}\end{bmatrix}, \tag{14}$$

where $\alpha_1 \in \mathbb{R}_{+}$ is a positive constant, shall be considered. Herein, the diagonal matrix $\boldsymbol{T}_{\mathrm{VR}}$ contains the equivalent time constants of the velocity-controlled robot and the positive definite diagonal matrix $\boldsymbol{K}_{\mathrm{P}}^{-1}$ specifies the inverse position controller gains. To show the positive definiteness of (14), Schurs‘ complement condition for positive definiteness (Serre, 2010) is applied. By doing this, it can be noticed that $V_{\mathrm{p}}(\boldsymbol{e}_{\mathrm{q}}, \dot{\boldsymbol{e}}_{\mathrm{q}})$ is positive definite, if the inequalities

$$\alpha_1\boldsymbol{K}_{\mathrm{P}}^{-1} \overset{!}{\succ} \boldsymbol{0}_{\mathrm{n}\times\mathrm{n}}, \tag{15a}$$

$$\boldsymbol{K}_{\mathrm{P}}^{-1}\boldsymbol{T}_{\mathrm{VR}} - \alpha_1(\boldsymbol{K}_{\mathrm{P}}^{-1}\boldsymbol{T}_{\mathrm{VR}})^{\top}\boldsymbol{K}_{\mathrm{P}}(\boldsymbol{K}_{\mathrm{P}}^{-1}\boldsymbol{T}_{\mathrm{VR}}) \overset{!}{\succ} \boldsymbol{0}_{\mathrm{n}\times\mathrm{n}}, \tag{15b}$$

are fulfilled. Therein, $\succ$ denotes positive definiteness of the corresponding matrices.

Note that (15a) is always true by construction. Since $\boldsymbol{K}_{\mathrm{P}}$ and $\boldsymbol{T}_{\mathrm{VR}}$ are defined as diagonal matrices with positive entries, (15b) can be simplified to

$$\boldsymbol{K}_{\mathrm{P}}^{-1}\boldsymbol{T}_{\mathrm{VR}}\left[\boldsymbol{I} - \alpha_1\boldsymbol{T}_{\mathrm{VR}}\right] \overset{!}{\succ} \boldsymbol{0}_{\mathrm{n}\times\mathrm{n}}. \tag{16}$$

Given (16), it can be observed that the inequality constraint can be satisfied choosing α_1, such that $\alpha_1\boldsymbol{I} \prec \boldsymbol{T}_{\mathrm{VR}}^{-1}$ holds. By doing this, $V_{\mathrm{p}}(\boldsymbol{e}_{\mathrm{q}}, \dot{\boldsymbol{e}}_{\mathrm{q}})$ is positive definite for any $\boldsymbol{e}_{\mathrm{q}}$, $\dot{\boldsymbol{e}}_{\mathrm{q}}$ in $\overline{\mathbb{Q}}_{\mathrm{R}} \times \mathbb{R}^{n}$. Further, regarding the stability conditions for time-varying systems, there always exist two time-invariant positive definite functions on $\overline{\mathbb{Q}}_{\mathrm{R}} \times \mathbb{R}^{n}$ that bound the Lyapunov function candidate, i.e., $W_{\mathrm{p},1}(\boldsymbol{e}_{\mathrm{q}}, \dot{\boldsymbol{e}}_{\mathrm{q}}) \le V_{\mathrm{p}}(\boldsymbol{e}_{\mathrm{q}}, \dot{\boldsymbol{e}}_{\mathrm{q}}) \le W_{\mathrm{p},2}(\boldsymbol{e}_{\mathrm{q}}, \dot{\boldsymbol{e}}_{\mathrm{q}})$.

The time derivative of the Lyapunov function candidate (14) along the solutions of (13) is given by

$$\dot{V}_{\mathrm{p}}(\boldsymbol{e}_{\mathrm{q}}, \dot{\boldsymbol{e}}_{\mathrm{q}}, t) = \begin{bmatrix}\boldsymbol{e}_{\mathrm{q}}\\ \dot{\boldsymbol{e}}_{\mathrm{q}}\end{bmatrix}^{\top}\underbrace{\begin{bmatrix}\alpha_1(\boldsymbol{S}^{\perp}\boldsymbol{J})^{+}(\boldsymbol{S}^{\perp}\boldsymbol{J}) & \frac{1}{2}(\boldsymbol{S}^{\perp}\boldsymbol{J})^{+}(\boldsymbol{S}^{\perp}\boldsymbol{J})\\ \frac{1}{2}(\boldsymbol{S}^{\perp}\boldsymbol{J})^{+}(\boldsymbol{S}^{\perp}\boldsymbol{J}) & \boldsymbol{K}_{\mathrm{P}}^{-1} - \alpha_1\boldsymbol{K}_{\mathrm{P}}^{-1}\boldsymbol{T}_{\mathrm{VR}}\end{bmatrix}}_{=:\boldsymbol{\Gamma}_{\dot{\mathrm{V}}_{\mathrm{p}}}}\begin{bmatrix}\boldsymbol{e}_{\mathrm{q}}\\ \dot{\boldsymbol{e}}_{\mathrm{q}}\end{bmatrix}. \tag{17}$$

In order to investigate the sign of $\dot{V}_{\mathrm{p}}(\boldsymbol{e}_{\mathrm{q}}, \dot{\boldsymbol{e}}_{\mathrm{q}}, t)$, Schurs' Lemma for positive semidefinite matrices is considered. With respect to the positive semidefiniteness of the projection matrix $(\boldsymbol{S}^{\perp}\boldsymbol{J}(\boldsymbol{e}_{\mathrm{q}}, t))^{+}(\boldsymbol{S}^{\perp}\boldsymbol{J}(\boldsymbol{e}_{\mathrm{q}}, t))$ (Fisher and Mujtaba, 1992) and the properties of generalized inverses/pseudoinverses (Serre, 2010), the matrix $\boldsymbol{\Gamma}_{\dot{\mathrm{V}}_{\mathrm{p}}}$ in (17) is positive semidefinite, if

$$\alpha_1^2\boldsymbol{K}_{\mathrm{P}}^{-1}\boldsymbol{T}_{\mathrm{VR}} - \alpha_1\boldsymbol{K}_{\mathrm{P}}^{-1} + \frac{1}{4}(\boldsymbol{S}^{\perp}\boldsymbol{J}(\boldsymbol{e}_{\mathrm{q}}, t))^{+}(\boldsymbol{S}^{\perp}\boldsymbol{J}(\boldsymbol{e}_{\mathrm{q}}, t)) \overset{!}{\preceq} \boldsymbol{0},$$

where similar to before $\prec$ is used to denote negative definiteness.

Since the projection matrix $(\boldsymbol{S}^{\perp}\boldsymbol{J}(\boldsymbol{e}_{\mathrm{q}}, t))^{+}(\boldsymbol{S}^{\perp}\boldsymbol{J}(\boldsymbol{e}_{\mathrm{q}}, t))$ represents a positive semidefinite matrix, it can be bounded using its smallest and largest eigenvalues, i.e., $\boldsymbol{0}_{\mathrm{n}\times\mathrm{n}} \preceq (\boldsymbol{S}^{\perp}\boldsymbol{J}(\boldsymbol{e}_{\mathrm{q}}, t))^{+}(\boldsymbol{S}^{\perp}\boldsymbol{J}(\boldsymbol{e}_{\mathrm{q}}, t)) \preceq \boldsymbol{I}$ concerning the idempotency property (Fisher and Mujtaba, 1992; Serre, 2010). Then, a sufficient condition for $\dot{V}_{\mathrm{p}}(\boldsymbol{e}_{\mathrm{q}}, \dot{\boldsymbol{e}}_{\mathrm{q}}, t)$ being negative semidefinite is given by the inequality constraint

$$\alpha_1^2\boldsymbol{K}_{\mathrm{P}}^{-1}\boldsymbol{T}_{\mathrm{VR}} - \alpha_1\boldsymbol{K}_{\mathrm{P}}^{-1} + \frac{1}{4}\boldsymbol{I} \overset{!}{\preceq} \boldsymbol{0}. \tag{18}$$

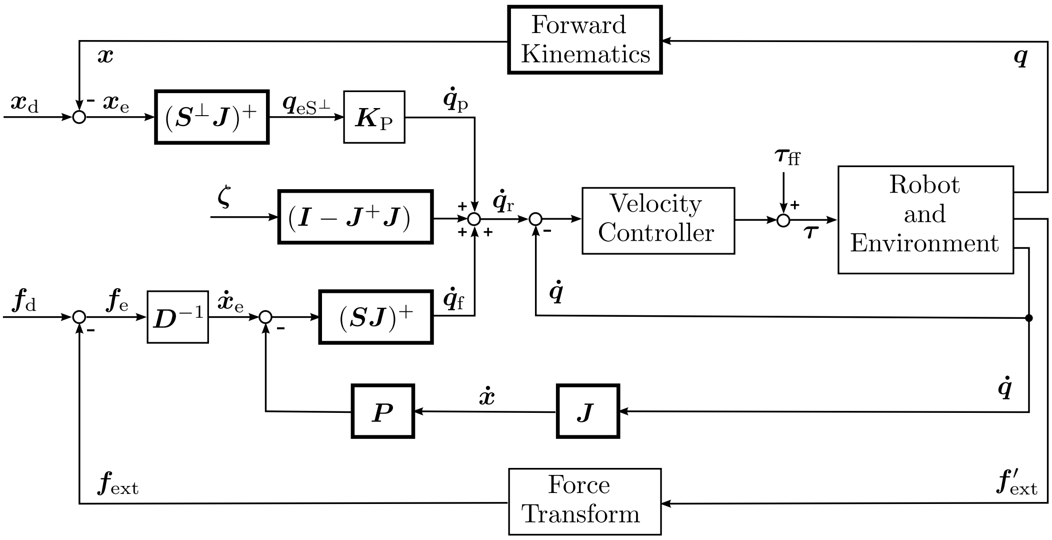

Fig. 1. Structure of the proposed velocity-based hybrid force/motion control scheme, where the modifications to the original structure are highlighted by bold blocks, i.e., the nonlinear proportional controllers $(\boldsymbol{SJ}(\boldsymbol{q}))^{+}\boldsymbol{D}^{-1}$ and $\boldsymbol{K}_{\mathrm{P}}(\boldsymbol{S}^{\perp}\boldsymbol{J}(\boldsymbol{q}))^{+}$, the additional Cartesian velocity feedback $\boldsymbol{PJ}$ and a null space input.

Solving the quadratic inequality (18) with respect to the parameter α_1, it can be observed, that the sufficient condition (18) is fulfilled choosing α_1 within a range of

$$\frac{1}{2}\boldsymbol{T}_{\mathrm{VR}}^{-1} - \frac{1}{2}\boldsymbol{T}_{\mathrm{VR}}^{-1}\sqrt{\boldsymbol{\Sigma}} \preceq \alpha_1 \boldsymbol{I} \preceq \frac{1}{2}\boldsymbol{T}_{\mathrm{VR}}^{-1} + \frac{1}{2}\boldsymbol{T}_{\mathrm{VR}}^{-1}\sqrt{\boldsymbol{\Sigma}}. \quad (19)$$

Here, $\boldsymbol{\Sigma} \in \mathbb{R}^{n\times n}$, $\boldsymbol{\Sigma} = \boldsymbol{I} - \boldsymbol{K}_{\mathrm{P}}\boldsymbol{T}_{\mathrm{VR}}$, which has to be positive semidefinite, i.e., $\boldsymbol{\Sigma} \succeq \boldsymbol{0}$, avoiding complex solutions of (19). Using (19) to select α_1 appropriately, simultaneously results in a positive definite Lyapunov function $V_{\mathrm{p}}(\boldsymbol{e}_{\mathrm{q}}, \dot{\boldsymbol{e}}_{\mathrm{q}})$ satisfying the condition (16).

With respect to present manipulators and high velocity controller bandwidths, it can be assumed that $T_{\mathrm{VR},i} \ll 1, \forall i$ in real applications. Therefore, it is possible to find a valid α_1 that satisfies (18) for proper choices of $\boldsymbol{K}_{\mathrm{P}}$. In particular, tuning the position controllers to achieve the same critically damped behavior for each position-controlled joint, i.e., $\boldsymbol{K}_{\mathrm{P}} = 1/4\boldsymbol{T}_{\mathrm{VR}}^{-1}$, the parameter α_1 can be chosen such that $1/2\boldsymbol{T}_{\mathrm{VR}}^{-1} - \sqrt{3}/4\boldsymbol{T}_{\mathrm{VR}}^{-1} \preceq \alpha_1\boldsymbol{I} \preceq 1/2\boldsymbol{T}_{\mathrm{VR}}^{-1} + \sqrt{3}/4\boldsymbol{T}_{\mathrm{VR}}^{-1}$.

Hence, the proposed Lyapunov function candidate (14) is a valid positive definite Lyapunov function with a negative semidefinite time derivative $\dot{V}_{\mathrm{p}}(\boldsymbol{e}_{\mathrm{q}}, \dot{\boldsymbol{e}}_{\mathrm{q}}, t) \le 0$ in $\overline{\mathbb{Q}}_{\mathrm{R}} \times \mathbb{R}^n$ for all $t \ge 0$ and proper choices of $\boldsymbol{K}_{\mathrm{P}}$ and α_1. According to the Lyapunov theory, it can be concluded that the equilibrium point $\left[\boldsymbol{e}_{\mathrm{q}}^{\top}, \dot{\boldsymbol{e}}_{\mathrm{q}}^{\top}\right]^{\top} = \boldsymbol{0}$ of the nonlinear system (13) is uniformly stable (Khalil, 2001).

In order to prove asymptotic stability, it is proposed to define the domain $\mathbb{D}_{\mathrm{p}} \subseteq \overline{\mathbb{Q}}_{\mathrm{R}} \subset \mathbb{R}^n$ as

$$\mathbb{D}_{\mathrm{p}} := \left\{\boldsymbol{\xi}_1 \in \overline{\mathbb{Q}}_{\mathrm{R}} \,|\, \exists \boldsymbol{e}_{\mathrm{q}} \in \overline{\mathbb{Q}}_{\mathrm{R}} : \boldsymbol{\xi}_1 = (\boldsymbol{S}^{\perp}\boldsymbol{J})^{+}(\boldsymbol{S}^{\perp}\boldsymbol{J})\boldsymbol{e}_{\mathrm{q}}\right\},$$

containing the origin $\boldsymbol{e}_{\mathrm{q}} = \boldsymbol{0}$. By doing this, projections onto the null space of $(\boldsymbol{S}^{\perp}\boldsymbol{J}(\boldsymbol{e}_{\mathrm{q}}, t))$ are excluded and only joint configurations resulting in end-effector movements in the Cartesian position-controlled directions are considered. [2]

Then, considering the supposed Lyapunov function (14) to be defined as $V_{\mathrm{p}}(\boldsymbol{e}_{\mathrm{q}}, \dot{\boldsymbol{e}}_{\mathrm{q}}) : \mathbb{D}_{\mathrm{p}} \times \mathbb{R}^n \mapsto \mathbb{R}$, the stability analysis can be performed with respect to the state variables $\boldsymbol{e}_{\mathrm{q}} \in \mathbb{D}_{\mathrm{p}}$, $\dot{\boldsymbol{e}}_{\mathrm{q}} \in \mathbb{R}^n$. Since the elements of the state variable $\boldsymbol{e}_{\mathrm{q}}$ are defined in the domain $\mathbb{D}_{\mathrm{p}}$, the projection matrix $(\boldsymbol{S}^{\perp}\boldsymbol{J}(\boldsymbol{e}_{\mathrm{q}}, t))^{+}(\boldsymbol{S}^{\perp}\boldsymbol{J}(\boldsymbol{e}_{\mathrm{q}}, t))$ represents a positive definite matrix (instead of a positive semidefinite matrix). As a consequence, using Schurs‘ complement condition, it can be observed that the matrix $\boldsymbol{\Gamma}_{\dot{\mathrm{V}}_{\mathrm{p}}}$ in (17) is positive definite for proper choices of $\boldsymbol{K}_{\mathrm{P}}$ and α_1.

Hence, the time derivative of the Lyapunov function $\dot{V}_{\mathrm{p}}(\boldsymbol{e}_{\mathrm{q}}, \dot{\boldsymbol{e}}_{\mathrm{q}}, t)$ is negative definite, i.e., $\dot{V}_{\mathrm{p}}(\boldsymbol{e}_{\mathrm{q}}, \dot{\boldsymbol{e}}_{\mathrm{q}}, t) \le -W_{\mathrm{p},3}(\boldsymbol{e}_{\mathrm{q}}, \dot{\boldsymbol{e}}_{\mathrm{q}}) < 0, \forall t \ge 0, \forall \boldsymbol{e}_{\mathrm{q}} \in \mathbb{D}_{\mathrm{p}}, \dot{\boldsymbol{e}}_{\mathrm{q}} \in \mathbb{R}^n$, and thus, the equilibrium point $\left[\boldsymbol{e}_{\mathrm{q}}^{\top}, \dot{\boldsymbol{e}}_{\mathrm{q}}^{\top}\right]^{\top} = \boldsymbol{0}$ of the nonlinear system (13) is UAS (in $\mathbb{D}_{\mathrm{p}} \times \mathbb{R}^n$).

Remark 4. The developed analysis is valid for any choice of the selection matrix $\boldsymbol{S}^{\perp} \ne \boldsymbol{0}$ and thus, does not necessarily require that $\boldsymbol{S}^{\perp} = \boldsymbol{I}, \boldsymbol{S} = \boldsymbol{0}$.

Passivity of the Force-Controlled Manipulator Considering the simplified robot model (6), the dynamics of the force-controlled manipulator in joint space w/o additional Cartesian velocity feedback, i.e $-\boldsymbol{P}\dot{\boldsymbol{x}}$, are given by

$$\frac{d}{dt}\dot{\boldsymbol{q}} = \boldsymbol{T}_{\mathrm{VR}}^{-1}\left[(\boldsymbol{SJ}(\boldsymbol{q}))^{+}\boldsymbol{D}^{-1}\boldsymbol{f}_{\mathrm{e}} + \left(\boldsymbol{I} - \boldsymbol{J}^{+}(\boldsymbol{q})\boldsymbol{J}(\boldsymbol{q})\right)\boldsymbol{\zeta} - \dot{\boldsymbol{q}}\right], \quad (20)$$

with the force error $\boldsymbol{f}_{\mathrm{e}} = \boldsymbol{f}_{\mathrm{d}}(t) - \boldsymbol{f}_{\mathrm{ext}}$ and null space vector $\boldsymbol{\zeta}$ as control input.

As can be observed, the system dynamics (20) directly depend on the state variable $\dot{\boldsymbol{q}}$, i.e., the joint velocities in joint space, while the control variable $\boldsymbol{f}_{\mathrm{ext}}(\boldsymbol{x})$ and thus the control input $\boldsymbol{f}_{\mathrm{e}}$ represents a position-dependent state in the Cartesian space. In order to avoid state variables of different spaces, it is convenient to express

[2] Since the matrix $(\boldsymbol{S}^{\perp}\boldsymbol{J}(\boldsymbol{e}_{\mathrm{q}}, t))$ is a continuous transformation and $(\boldsymbol{S}^{\perp}\boldsymbol{J}(\boldsymbol{e}_{\mathrm{q}}, t))^{+}(\boldsymbol{S}^{\perp}\boldsymbol{J}(\boldsymbol{e}_{\mathrm{q}}, t))$ represents a bijective transformation on the set $\overline{\mathbb{Q}}_{\mathrm{R}} \setminus \boldsymbol{e}_{\mathrm{q}} \in \ker((\boldsymbol{S}^{\perp}\boldsymbol{J})^{+}(\boldsymbol{S}^{\perp}\boldsymbol{J}))$, it can be assumed that $\mathbb{D}_{\mathrm{p}}$ is a partition of the set $\overline{\mathbb{Q}}_{\mathrm{R}}$, which does not contain any unit sets. Thus, the set $\mathbb{D}_{\mathrm{p}} \subset \mathbb{R}^n$ can be used in the stability analysis according to the Lyapunov theory (Khatib, 1995).

the Cartesian force error $\boldsymbol{f}_{\mathrm{e}}$ in terms of joint torques using the dynamically consistent generalized inverse of (5), i.e., $\boldsymbol{f}_{\mathrm{e}} = \boldsymbol{J}^{T\#}(\boldsymbol{q})\boldsymbol{\tau}_{\mathrm{e}}$, $\boldsymbol{\tau}_{\mathrm{e}} \in \mathbb{R}^n$, so that (20) becomes

$$\frac{d}{dt}\dot{\boldsymbol{q}} = \boldsymbol{T}_{\mathrm{VR}}^{-1}\left[(\boldsymbol{SJ}(\boldsymbol{q}))^{+}\boldsymbol{D}^{-1}\boldsymbol{J}^{T\#}(\boldsymbol{q})\boldsymbol{\tau}_{\mathrm{e}} + \left(\boldsymbol{I} - \boldsymbol{J}^{+}(\boldsymbol{q})\boldsymbol{J}(\boldsymbol{q})\right)\boldsymbol{\zeta} - \dot{\boldsymbol{q}}\right]. \tag{21}$$

Referring to the passivity definition, the following non-negative (time-invariant) storage function $S_{\mathrm{f}}(\dot{\boldsymbol{q}}) : \mathbb{R}^n \mapsto \mathbb{R}$,

$$S_{\mathrm{f}}(\dot{\boldsymbol{q}}) = \frac{1}{2}\alpha_2 \dot{\boldsymbol{q}}^T \boldsymbol{T}_{\mathrm{VR}} \dot{\boldsymbol{q}}, \tag{22}$$

is considered, where $\alpha_2 \in \mathbb{R}_+$ is a positive constant. Thus, the time derivative of $S_{\mathrm{f}}(\dot{\boldsymbol{q}})$ along the solutions of (21) is given by

$$\dot{S}_{\mathrm{f}}(\boldsymbol{q}, \dot{\boldsymbol{q}}) = \alpha_2 \dot{\boldsymbol{q}}^T (\boldsymbol{SJ}(\boldsymbol{q}))^{+}\boldsymbol{D}^{-1}\boldsymbol{J}^{T\#}(\boldsymbol{q})\boldsymbol{\tau}_{\mathrm{e}} - \alpha_2 \dot{\boldsymbol{q}}^T\dot{\boldsymbol{q}} + \alpha_2 \dot{\boldsymbol{q}}^T\left(\boldsymbol{I} - \boldsymbol{J}^{+}(\boldsymbol{q})\boldsymbol{J}(\boldsymbol{q})\right)\boldsymbol{\zeta}. \tag{23}$$

Since the transformation matrix

$$(\boldsymbol{SJ}(\boldsymbol{q}))^{+}\boldsymbol{J}(\boldsymbol{q}) = (\boldsymbol{SJ}(\boldsymbol{q}))^{+}(\boldsymbol{SJ}(\boldsymbol{q}))$$

(Fisher and Mujtaba, 1992), the matrix

$$(\boldsymbol{SJ}(\boldsymbol{q}))^{+}\boldsymbol{D}^{-1}\boldsymbol{J}^{T\#}(\boldsymbol{q}) = (\boldsymbol{SJ}(\boldsymbol{q}))^{+}(\boldsymbol{SJ}(\boldsymbol{q}))\boldsymbol{J}^{\#}(\boldsymbol{q})\boldsymbol{D}^{-1}\boldsymbol{J}^{T\#}(\boldsymbol{q}),$$

where $\boldsymbol{J}^{\#}(\boldsymbol{q})$ is used as a special generalized (right) inverse, satisfying $\boldsymbol{J}(\boldsymbol{q})\boldsymbol{J}^{\#}(\boldsymbol{q}) = \boldsymbol{I}$. The first part $(\boldsymbol{SJ}(\boldsymbol{q}))^{+}(\boldsymbol{SJ}(\boldsymbol{q}))$ defines a projection matrix and

$$\boldsymbol{J}^{\#}(\boldsymbol{q})\boldsymbol{D}^{-1}\boldsymbol{J}^{T\#}(\boldsymbol{q})$$

represents a positive definite matrix for positive definite inverse damping matrices $\boldsymbol{D}^{-1}$ (Serre, 2010). Since, according to the idempotency property (Fisher and Mujtaba, 1992; Serre, 2010), per definition, the largest eigenvalue of any projection matrix is 1 and thus, the largest singular value is also 1, the matrix $(\boldsymbol{SJ}(\boldsymbol{q}))^{+}\boldsymbol{D}^{-1}\boldsymbol{J}^{T\#}(\boldsymbol{q})$ can be bounded from above using the induced spectral norm, i.e.,

$$\left\|(\boldsymbol{SJ}(\boldsymbol{q}))^{+}\boldsymbol{D}^{-1}\boldsymbol{J}^{T\#}(\boldsymbol{q})\right\|_2 \leq \sup_{\boldsymbol{q}\in\overline{\mathbb{Q}}_{\mathrm{R}}} \sigma_{\max}(\boldsymbol{J}^{\#}(\boldsymbol{q})\boldsymbol{D}^{-1}\boldsymbol{J}^{T\#}(\boldsymbol{q})) < \infty, \tag{24}$$

considering the boundedness properties of the Jacobian $\boldsymbol{J}(\boldsymbol{q})$ in the non-singular space. Hence, it is always possible to specify a controller gain matrix $\boldsymbol{D}^{-1}$ and find an α_2, such that the inequality constraint

$$\alpha_2 \left\|(\boldsymbol{SJ}(\boldsymbol{q}))^{+}\boldsymbol{D}^{-1}\boldsymbol{J}^{T\#}(\boldsymbol{q})\right\|_2 \leq 1, \qquad \boldsymbol{q} \in \overline{\mathbb{Q}}_{\mathrm{R}}, \tag{25}$$

is fulfilled, e.g., by selecting

$$\alpha_2 = \sup\left[\sigma_{\max}(\boldsymbol{J}^{\#}(\boldsymbol{q})\boldsymbol{D}^{-1}\boldsymbol{J}^{T\#}(\boldsymbol{q}))\right]^{-1}, \boldsymbol{q} \in \overline{\mathbb{Q}}_{\mathrm{R}}.$$

Note that, the inverse damping matrix $\boldsymbol{D}^{-1}$ usually satisfies $\left\|\boldsymbol{D}^{-1}\right\| \ll 1$ in real applications involving stiff environments. As a consequence, choosing an appropriate α_2 and a $\boldsymbol{\zeta}$ satisfying $\|\boldsymbol{\zeta}\| \leq \|\dot{\boldsymbol{q}}\|$, the time derivative $\dot{S}_{\mathrm{f}}(\boldsymbol{q}, \dot{\boldsymbol{q}})$ of (23) can be bounded by

$$\dot{S}_{\mathrm{f}}(\boldsymbol{q}, \dot{\boldsymbol{q}}) \leq \dot{\boldsymbol{q}}^{\top}\boldsymbol{\tau}_{\mathrm{e}} - \alpha_2\dot{\boldsymbol{q}}^T\dot{\boldsymbol{q}} + \alpha_2\dot{\boldsymbol{q}}^T\left(\boldsymbol{I} - \boldsymbol{J}^{+}(\boldsymbol{q})\boldsymbol{J}(\boldsymbol{q})\right)\boldsymbol{\zeta}, \tag{26}$$

with $\|\boldsymbol{\zeta}\| \leq \|\dot{\boldsymbol{q}}\|$ for any $\boldsymbol{q} \in \overline{\mathbb{Q}}_{\mathrm{R}}$ and $\dot{\boldsymbol{q}} \in \mathbb{R}^n$.

Considering the differential dissipation inequality and the passivity definition (Khalil, 2001), given (26), it can be concluded that the nonlinear system (21) is passive with respect to the supply rate $s(\boldsymbol{\tau}_{\mathrm{e}}, \dot{\boldsymbol{q}}) = \dot{\boldsymbol{q}}^{\top}\boldsymbol{\tau}_{\mathrm{e}}$, where $\boldsymbol{\tau}_{\mathrm{e}}$ corresponds to the input $\boldsymbol{u}$ and $\dot{\boldsymbol{q}}$ corresponds to the system output $\boldsymbol{y}$. Furthermore, considering the positive definiteness of the projection matrix $(\boldsymbol{I} - \boldsymbol{J}^{+}(\boldsymbol{q})\boldsymbol{J}(\boldsymbol{q}))$, if $\|\boldsymbol{\zeta}\| < \|\dot{\boldsymbol{q}}\|$, the system is output strictly passive. Hence, in case of the trivial null space treatment $\boldsymbol{\zeta} = \boldsymbol{0}$, the nonlinear system (21) is output strictly passive.

Stability of the Force-Controlled Manipulator Since the proposed storage function (22) represents a positive definite function of the state $\dot{\boldsymbol{q}}$, the equilibrium point $\dot{\boldsymbol{q}} = \boldsymbol{0}$ of the (unforced/ autonomous) nonlinear, passive system (21) with input $\boldsymbol{\tau}_{\mathrm{e}} = \boldsymbol{0}$ is stable in the sense of Lyapunov. Moreover, choosing an appropriate $\boldsymbol{\zeta}$ such that the system is (output) strictly passive, e.g., $\boldsymbol{\zeta} = \boldsymbol{0}$, asymptotic stability of the origin $\boldsymbol{0}$ can be concluded.

Furthermore, using the properties of passive systems, the purely force-controlled manipulator interacting with its environment can be understood as an interconnection of passive subsystems, where the passive environment describes a mapping of the form $\dot{\boldsymbol{q}} \to \boldsymbol{f}_{\mathrm{ext}}$ (Ott, 2008). Thus, the overall system is passive. Particularly, the environment can be assumed to be strictly passive, which is valid considering the environment as a connection of passive (e.g., springs) and dissipative/strictly passive (e.g., dampers) elements (Hogan and Buerger, 2005). It can be concluded that the equilibrium point $\dot{\boldsymbol{q}} = \boldsymbol{0}$ of the feedback interconnection of the strictly passive force-controlled manipulator and a strictly passive environment is (globally) asymptotically stable for the reference signal $\boldsymbol{\tau}_{\mathrm{d}} = \boldsymbol{0}$.

Concerning the modified hybrid control structure of Fig. 1, an additional feedback part $-\boldsymbol{PJ}(\boldsymbol{q})\dot{\boldsymbol{q}}$ is supposed in order to add extra damping to the force-controlled system in case of an environmental interaction. This controller can be represented by the equivalent feedback $-\boldsymbol{J}^T(\boldsymbol{q})\boldsymbol{DPJ}(\boldsymbol{q})\dot{\boldsymbol{q}}$, which is a (mathematical) extension to close the feedback-loop using $\boldsymbol{J}^T(\boldsymbol{q})$ as right inverse of $\boldsymbol{J}^{T\#}(\boldsymbol{q})$. It interconnects the passive manipulator and the passive environment. As can be observed from the previous analysis, the modification is not mandatory in terms of achieving (asymptotic) stability, but improves the dynamic closed-loop behavior by dissipating energy (especially in case of an unexpected impact). Thus, intuitively, the additional feedback part cannot destabilize the closed-loop system. On the contrary, considering the concept of asymptotically stabilizing a nonlinear passive system by means of output feedback (Byrnes et al., 1991), the extension can be interpreted as a controller of the form

$$\boldsymbol{\tau}_{\mathrm{e}} = -\boldsymbol{\Phi}(\dot{\boldsymbol{q}}) = -\boldsymbol{J}^T(\boldsymbol{q})\boldsymbol{DPJ}(\boldsymbol{q})\dot{\boldsymbol{q}}. \tag{27}$$

Herein, the matrix $\boldsymbol{J}^T(\boldsymbol{q})\boldsymbol{DPJ}(\boldsymbol{q})$ represents a smooth transformation, that can be designed to be positive definite, e.g., choosing $\boldsymbol{D}^{-1}$ and $\boldsymbol{P}$ as diagonal matrices with positive elements. Since the interconnection of the force-controlled manipulator with a strictly passive environment is asymptotically stable (and thus zero-state detectable), the control law (27) ensures the asymptotic stability of the origin $\boldsymbol{0}$ and acts stabilizing additionally. Furthermore, it can be assumed that the controller implies beneficial robustness properties.

Remark 5. These results confirm the investigations of Colgate and Hogan (1988). Using transfer functions and the Nyquist stability criterion, they showed that a passive manipulator interacting with a passive environment is stable. Moreover, the closed-loop system is asymptotically stable if either of the two systems is strictly passive (Hogan and Buerger, 2005; Colgate and Hogan, 1988).

In general, the target behavior during a manipulator-environment-interaction can be chosen arbitrary to fulfill certain criteria. From a practical point of view, it is beneficial to specify the desired dynamics dependent on the environmental characteristics and the manipulator properties, such as the stiffness of the end-effector tool gripping a workpiece. In this way, a priori knowledge of the material stiffness and damping involved in the assembly task are taken into account. Details of the design approach are beyond the scope of this paper, but are included in (Hans, 2015).

5. APPLICATION

For showing the effectiveness of the proposed approach, an environmental interaction scenario is sketched using ABB's collaborative robot YuMi® . It is a dual-arm, redundant robot with 7 DoF on each arm that is designed for small parts assembly and safe human robot collaboration. It has a handling capacity of 500 g (including the gripper) and a maximum task-space velocity of $1.5\,\mathrm{m\,s^{-1}}$. Given these specifications we will use it to charge soft and guided springs showcasing the performance of the proposed modifications for controlling environmental interaction.

The modified hybrid control scheme sketched in Fig. 1 was implemented utilizing the (factory) settings of the inner velocity controller and position controller gain matrix $\boldsymbol{K}_\mathrm{P}$. The remaining structure parts were supported by the measured joint configuration $\boldsymbol{q}$ and joint velocity $\dot{\boldsymbol{q}}$ within a sample period of $T_\mathrm{s} = 0.04\,\mathrm{s}$, respectively. The exerted forces were measured using a wrist-mounted force/torque sensor. This is assembled below a gripper, that defined the tool center point of the robot end-effector.

The experimental setup is depicted in Fig. 2. The purely position-controlled manipulator, i.e., $\boldsymbol{S}^\perp = \boldsymbol{I}_{6\times6}$, $\boldsymbol{\zeta} = \boldsymbol{0}$, tracks a pre-calculated reference trajectory $\boldsymbol{q}_\mathrm{d}(t)$ (generated by an integrated controller unit) that is transformed to Cartesian space using the forward kinematics $\boldsymbol{x}_\mathrm{d}(t) = \mathcal{K}(\boldsymbol{q}_\mathrm{d}(t))$. After exceeding a force threshold/dead zone of $|f_{\mathrm{text},z}| = 0.3\,\mathrm{N}$,, the controller is switched to force control in the constrained direction setting $S_z = 1$, and $\boldsymbol{f}_\mathrm{d}(t) = \boldsymbol{0}\mathrm{N}$.

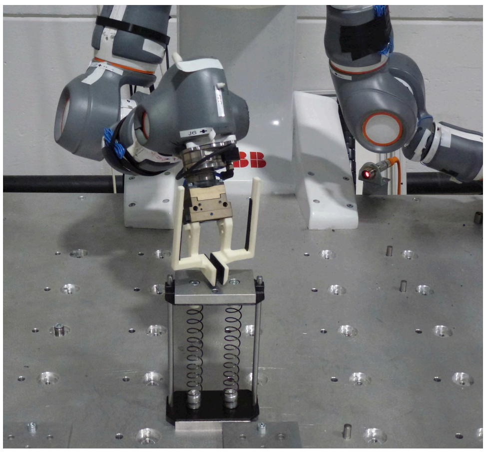

Fig. 2. Experimental setup with end-effector motion in the Cartesian z-direction hitting an unexpected environment with stiffness $K_\mathrm{e} = 1000\,\mathrm{N\,m^{-1}}$.

Utilizing a priori knowledge of the equivalent time constants $\boldsymbol{T}_\mathrm{VR}$ and the environmental stiffness, the measured end-effector positions and exerted force evolutions are plotted in Fig. 3 through Fig. 5 for different force controller designs. The force controller with $D = 40\,\mathrm{N\,s\,m^{-1}}$ tuned empirically, results in the evolutions of Fig. 3 and shows a satisfactory interaction behavior. The exerted force decreases to zero with an overlaid oscillation. However, it can be imagined that an inappropriately chosen force controller gain matrix induces an oscillating behavior which could result in an undesired bouncing of the end-effector on the surface. In particular, a reduction of the gains to $D = 5\,\mathrm{N\,s\,m^{-1}}$ yields the predicted bouncing behavior as shown in Fig. 4. Therefore, an improper empirical design could lead to damage to the involved parts and often involves additional attrition, which represent the drawbacks of the simple trial and error design method. Moreover, an overly conservative gain choice yields an overcritically damped behavior and thus, increased settling times and exerted forces. On the other hand, short settling time can be achieved if a bouncing behavior is accepted. Furthermore, if successful tuning was accomplished once, the obtained parameters can readily be utilized as reference values in similar applications. Such trial and error approaches describe the typical process of tuning robot behavior in applications.

Fig. 5 shows the respective position and force evolutions using the proper design method mentioned earlier (Hans, 2015). Here, the controller is tuned to result in a critically damped system. Thus, the resulting force (Fig. 5) shows an approximately critically damped behavior. However, at this point, it should be highlighted that this design method targets the automatic parameterization for reducing oscillations, ending up with higher forces in some configurations. In doing so, bouncing effects are avoided and advantageous robustness properties can be deduced with respect to uncertain stiffness estimates as well as the errors resulting from the approximated velocity-controlled robot behavior (first-order lag). These results strengthen a possible application in small parts assembly.

6. CONCLUSION

In this article we revisited the classical problem of hybrid force/motion control of manipulators and showed how to improve applicability of such hybrid schemes in practical applications for both redundant and standard 6 DoF manipulators.

Basically, this is achieved using an in-depth stability analysis of the scheme leading to the introduction of an additional feedback component for its robustification. Furthermore, a design guideline is developed for tuning the repsective controller parameters to achieve satisfactory behavior. The effectiveness is then shown in a relevant environmental interaction scenario involving the redundant industrial manipulator YuMi® .

For the future, the authors seek to compare this setting with other interaction-control architectures based on impedance- or admittance-like approaches (e.g., Schindlbeck and Haddadin (2015); Wahrburg and Listmann (2016); Matschek et al. (2017)) in terms of robustness to imperfections in the task-space and task performance.

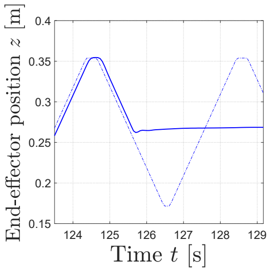

(a) End-effector position

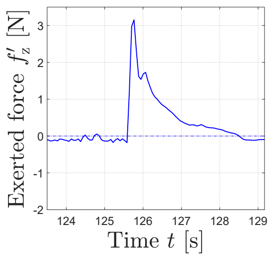

(b) Exerted force

Fig. 3. Position and force measurements in setup 1 using the trial and error method ($D_z = 40\,\mathrm{N\,s\,m^{-1}}$) showing a damped interaction behavior with risk to oscillations (dashed lines show references).

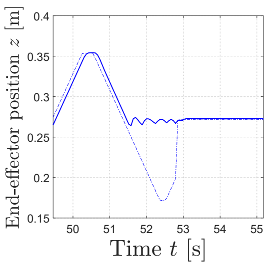

(a) End-effector position

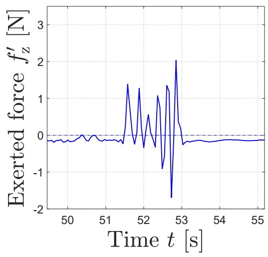

(b) Exerted force

Fig. 4. Position and force measurements in setup 1 using the trial and error method ($D_z = 5\,\mathrm{N\,s\,m^{-1}}$) showing an unstable bouncing interaction with the environment (dashed lines show references).

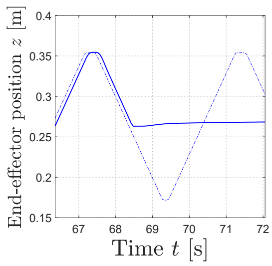

(a) End-effector position

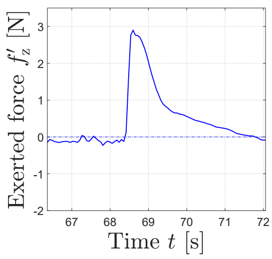

(b) Exerted force

Fig. 5. Position and force measurements in setup 1 using the generalized eigenvalue approach ($\delta_{\Lambda_T,z} = 1$) showing a critically damped interaction with a minimum of exerted force (dashed lines show references).

REFERENCES

An, C.H. and Hollerbach, J.M. (1987). Kinematic stability issues in force control of manipulators. In *Proc. 1987 IEEE Int. Conf. Robot. Autom.*, 897–903.

Brogårdh, T. (2009). Robot control overview: An industrial perspective. *Modeling, Identification and Control*, 30(3), 167.

Byrnes, C., Isidori, A., Willems, J.C., et al. (1991). Passivity, feedback equivalence, and the global stabilization of minimum phase nonlinear systems. *IEEE Trans. Autom. Control*, 36(11), 1228–1240.

Colgate, J.E. and Hogan, N. (1988). Robust control of dynamically interacting systems. *Int. J. Control*, 48(1), 65–88.

Craig, J.J. and Raibert, M.H. (1979). A systematic method of hybrid position/force control of a manipulator. In *Proc. IEEE Int. Comput. Softw. Appl. Conf.*, 446–451.

Fisher, W.D. and Mujtaba, M.S. (1992). Hybrid position/force control: a correct formulation. *Int. J. Robot. Research*, 11(4), 299–311.

Hans, F. (2015). *Compliant Control for Robust Assembly with Redundant Manipulators in Partially Unstructured Environments*. Master's thesis, Technische Universität München.

Hogan, N. (1985). Impedance control: An approach to manipulation: Part i-theory, part ii-implementation, part iii-applications. *J. Dyn. Sys., Meas., Control*, 107(1), 1–24.

Hogan, N. and Buerger, S.P. (2005). Impedance and interaction control. In T.R. Kurfess (ed.), *Robotics and Automation Handbook*, chapter 19, 1–24. CRC Press.

Jonsson, M., Stolt, A., Robertsson, A., von Gegerfelt, S., and Nilsson, K. (2013). On force control for assembly and deburring of castings. *Production Engineering Research and Development*, 7, 351–360.

Khalil, H. (2001). *Nonlinear Systems*. Prentice-Hall, 3rd edition.

Khatib, O. (1995). Inertial properties in robotic manipulation: An object-level framework. *Int. J. Robot. Research*, 14(1), 19–36.

Krüger, J., Lien, T., and Verl, A. (2009). Cooperation of human and machines in assembly lines. *CIRP Annals - Manuf. Technol.*, 58(2), 628–646.

Matschek, J., Bethge, J., Zometa, P., and Findeisen, R. (2017). Force feedback and path following using predictive control: Concept and application to a lightweight robot. *IFAC PapersOnLine*, 50(1), 9827–9832.

Ott, C., Mukherjee, R., and Nakamura, Y. (2010). Unified impedance and admittance control. In *Proc. 2010 IEEE Int. Conf. Robot. Autom.*, 554–561.

Ott, C. (2008). *Cartesian impedance control of redundant and flexible-joint robots*. Springer.

Schindlbeck, C. and Haddadin, S. (2015). Unified passivity-based cartesian force/impedance control for rigid and flexible joint robots via task-energy tanks. In *Proc. 2015 IEEE Int. Conf. Rob. Autom.*, 440–447.

Serre, D. (2010). *Matrices: Theory and Applications, volume 216 of Graduate Texts in Mathematics*. Springer-Verlag, New York.

Siciliano, B. and Villani, L. (1999). *Robot Force Control*. Kluwer Academic Publishers.

Siciliano, B. and Khatib, O. (2016). *Springer handbook of robotics*. Springer.

Spong, M.W. and Vidyasagar, M. (2008). *Robot Dynamics and Control*. John Wiley & Sons.

Thomas, C., Matthias, B., and Kuhlenkötter, B. (2016). Human robot collaboration – new applications in industrial robotics. In *Int. Conf. Comp. Manuf.*, 293–299.

Wahrburg, A. and Listmann, K. (2016). MPC-based admittance control for robotic manipulators. In *Proc. 55th IEEE Conf. Dec. Control*, 7548–7554.

Zeng, G. and Hemami, A. (1997). An overview on robot force control. *Robotica*, 15(5), 473–482.